EDGEWOOD

RESEARCH, DEVELOPMENT & ENGINEERING CENTER

U.S. ARMY CHEMICAL AND BIOLOGICAL DEFENSE COMMAND

ERDEC-TR-317

EVALUATION OF POST-TREATMENT FILTER

PART 2:   MODELING LABORATORY-SCALE FILTER BREAKTHROUGH DATA
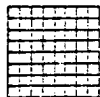
David T. Croft
David K. Friday

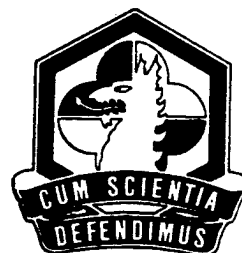GUILD ASSOCIATES, INCORPORATED
Baltimore, MD 21236

John J. Mahle

RESEARCH AND TECHNOLOGY DIRECTORATE

November 1996

Guild
Associates, Inc.

CUM SCIENTIA
DEFENDIMUS

Aberdeen Proving Ground, MD   21010-5423

19970124 100

DTIC QUALITY INSPECTED 3

Disclaimer

The findings in this report are not to be construed as an official Department of the Army position unless so designated by other authorizing documents.

REPORT DOCUMENTATION PAGE

1. AGENCY USE ONLY (Leave blank)	2. REPORT DATE 1996 November	3. REPORT TYPE AND DATES COVERED Final, 95 Mar - 95 Nov

4. TITLE AND SUBTITLE

Evaluation of Post-Treatment Filter, Part 2: Modeling Laboratory-Scale Filter Breakthrough Data

5. FUNDING NUMBERS

PR-1O262622A552

6. AUTHOR(S)

Croft, David T.; Friday, David K. (Guild Associates, Incorporated); and Mahle, John J. (ERDEC)

7. PERFORMING ORGANIZATION NAME(S) AND ADDRESS(ES)

DIR, ERDEC, ATTN: SCBRD-RTE, APG, MD 21010-5423
Guild Associates, Incorporated, 5022 Campbell Drive,
Suites J & K, Baltimore, MD 21236

8. PERFORMING ORGANIZATION REPORT NUMBER

ERDEC-TR-317

9. SPONSORING/MONITORING AGENCY NAME(S) AND ADDRESS(ES)

10. SPONSORING/MONITORING AGENCY REPORT NUMBER

11. SUPPLEMENTARY NOTES

12a. DISTRIBUTION/AVAILABILITY STATEMENT

Approved for public release; distribution is unlimited.

12b. DISTRIBUTION CODE

13. ABSTRACT (Maximum 200 words)

This report describes efforts to predict breakthrough of various challenge chemicals for the Post Treatment Filter (PTF) of the Pollution Abatement System (PAS). The work consisted of evaluating breakthrough data for the DMMP/coconut shell carbon breakthrough experiments of Mahle and Buettner; fitting model parameters to selected experimental data and finding and/or developing correlations for model parameters; and comparing predicted model parameter values to fitted results. Emphasis is on early breakthrough (low concentration) because of its importance in PTF evaluation, although the entire breakthrough curve is considered.

14. SUBJECT TERMS

High temperature breakthrough
Adsorption dynamics
Axial dispersion

15. NUMBER OF PAGES

25

16. PRICE CODE

17. SECURITY CLASSIFICATION OF REPORT UNCLASSIFIED	18. SECURITY CLASSIFICATION OF THIS PAGE UNCLASSIFIED	19. SECURITY CLASSIFICATION OF ABSTRACT UNCLASSIFIED	20. LIMITATION OF ABSTRACT UL

Blank

PREFACE

The work described in this report was authorized under Project No. 1O262622A552, Smoke Obscurants/Munitions. This work was started in March 1995 and completed in November 1995.

The use of trade or manufacturers' names in this report does not constitute an official endorsement of any commercial products. This report may not be cited for purposes of advertisement.

This report has been approved for public release. Registered users should request additional copies from the Defense Technical Information Center; unregistered users should direct such requests to the National Technical Information Service.

DTIC QUALITY INSPECTED 8

3

Blank

CONTENTS

FIGURES

TABLES

Evaluation of Post-Treatment Filter
PART 2. Modeling Laboratory-Scale Filter Breakthrough Data

1. INTRODUCTION

The Post-Treatment Filter (PTF) may serve to reduce pollutants during normal operation of the Pollution Abatement System (PAS) or, in the unlikely event of PAS failure, serve as a final containment system to prevent accidental release of toxins to the environment. The purpose of the modeling work is to enable prediction of the PTF performance under normal operating conditions and during a maximum credible event such as an incinerator burnout or explosion.

The useful life of an adsorptive filter depends (1) on its total capacity to adsorb a challenge chemical and (2) on the way in which the total capacity is approached. Considering the filter's capacity alone, premature breakthrough may drastically reduce its useful life relative to what would be expected. This premature breakthrough results from dispersion of the concentration wave as it passes through the filter. An understanding of adsorption equilibrium and dispersion are both crucial to correctly estimate filter performance.

The approach taken to evaluate the PTF incorporates estimates of adsorption equilibria, modeling breakthrough experiments on a laboratory-scale filter, and scaling up laboratory-scale results to the full-sized system. Adsorption equilibrium can be measured in the laboratory with little concern for scale-up problems. Conversely, the extent of premature breakthrough may differ depending on the size and shape of a filter, the flow rates, and other factors. Predicting the extent of early breakthrough from laboratory scale tests requires a detailed understanding of the factors that contribute to concentration wave spreading.

Many factors can influence dispersion in packed-bed filters. Studies of dispersion in beds with inert packing such as glass beads have been conducted.[1,2,3] Correlations for dispersion, considering interstitial fluid phenomena such as molecular diffusion, eddy dispersion, and radial velocity gradients have been developed and tested.[1,3] Mass transfer into adsorbent particles has also been studied extensively for the interparticle and intraparticle space, and methods for modeling these in adsorption beds are well established.[4]

Published studies on the effect adsorption has on dispersion are rare. Mahle and Friday[5] studied breakthrough of various challenge chemicals for the same adsorption bed. Measured data was modeled using a convection-diffusion equation. Langer and co-workers' correlation[3] was used to estimate effective dispersion coefficients. Measured mass transfer coefficients were used. The Langer correlation made good predictions only when the adsorption equilibrium was linear. The predictions were poor for favorably adsorbed chemicals. The convection-diffusion model used by Mahle and Friday[5] with an effective dispersion coefficient determined by the Langer correlation[3] predicts a sharpening of the breakthrough curve with a favorable isotherm. This was not observed experimentally.

Dispersion of interstitial fluid largely results from deviations from plug flow (a dependence of axial velocity on position on a radial cross-section). Langer and co-workers[3] showed experimentally that it depended on fixed-bed dimensions for beds with inert packing. To better understand the adsorption and bed dimension effects, a scale-up model, which considers radial dependency of the axial velocity, will be discussed.

The goal of the on-going work is to develop a set of model equations, which can be solved and thus used to evaluate the PTF. A subordinate goal is to develop a set of correlations, which will allow adsorber performance to be predicted, while requiring a minimum of data to be input to the model. The combined effects of adsorption and nonuniform flow (radial velocity gradients) may be important in determining the shape of the concentration breakthrough. This initial modeling effort (Part 2) involves maximum likelihood model parameter estimation using laboratory-scale experimental data, *a priori* estimation of model parameters, and comparing estimated parameters to fit parameters. Part 2 efforts will be followed by an estimation of scale-up effects. The final report will include the estimates of adsorption equilibria for the chemicals of interest and model predictions of the breakthrough times.

2.   THEORY

Two models were developed for predicting breakthrough behavior. The first is used to fit experimental data and to make breakthrough predictions. The second model is used to determine the dimensionless groups important in developing correlations to describe dispersion with adsorption. If the model is valid, the dimensionless groups derived from it should be useful in designing experiments, which may provide information relevant to a full-scale process. The dimensional analysis also will aid in developing a correlation for the effective dispersion coefficient of the first model, which considers adsorption and scale-up.

2.1   Breakthrough Model.

The model to be used for the final evaluation process will be referred to as the breakthrough model. It consists of a material balance neglecting fluid-phase accumulation,

$$\rho_b \frac{\partial q}{\partial t} + \frac{\partial \varepsilon\, v c}{\partial z} - D_L \frac{\partial^2 \varepsilon\, c}{\partial z^2} = 0 \tag{1}$$

a rate equation,

$$\rho_b \frac{\partial q}{\partial t} = k_f\, a\left(c - c^*\right) \tag{2}$$

and an adsorption equilibrium equation,

8

$$q = f(c^*, T) \tag{3}$$

where D_L is an effective axial dispersion coefficient, k_f is the external film mass transfer coefficient, a is the area per unit volume, and c^* is the vapor-phase concentration in equilibrium with the adsorbed phase. Intraparticle mass transfer resistance is neglected.

Wakao and Funazkri[6] give the following correlation to obtain the external mass transfer coefficient, k_f,

$$\frac{k_f d_p}{D_{AB}} = 2.0 + 1.1 \left[\frac{\varepsilon v \rho d_p}{\mu}\right]^{0.6} \left[\frac{\mu}{D_{AB} \rho}\right]^{0.333} \tag{4}$$

where d_p is the particle diameter assuming spherical particles, D_{AB} is the diffusivity of the chemical in the mixture, ρ is the vapor-phase density, and μ is the viscosity of the vapor-phase. The term εv is equivalent to Q/A where Q is the volumetric flow rate, and A is the cross-sectional area of the bed. For nonspherical particles, the particle diameter may be multiplied by a shape factor, ϕ_s.

A correlation for the effective dispersion coefficient is taken from Bischoff[1]

$$\frac{D_L}{\varepsilon v d_p} = \gamma \frac{D_{AB}}{\varepsilon v d_p} + \frac{0.45}{1 + \beta \gamma \frac{D_{AB}}{\varepsilon v d_p}} \tag{5}$$

where γ is a tortuosity factor equal to 0.73 and β is set equal to 10. This equation is based on work by Bischoff and Levenspiel,[7] who discussed the relationship between various dispersion models. The first term on the right accounts for molecular diffusion in the axial direction. The second term on the right accounts for dispersion due to nonuniform flow and the decreased dispersion due to radial diffusion and mixing.

Bischoff and Levenspiel[7] did not consider the effects of favorable adsorption. Determining a correction factor for favorable adsorption for Equation 5 is one objective of this work. Mahle and Friday[5] suggest dividing Langer and co-workers' correlation by the separation factor, R. In this report, the following correlation is tentatively proposed

$$\frac{D_L}{\varepsilon v d_p} = \gamma \frac{D_{AB}}{\varepsilon v d_p} + \frac{1}{R_1^n} \frac{0.45}{1 + \beta \gamma \frac{D_{AB}}{\varepsilon v d_p}} \tag{6}$$

were R_1 is related to the separation factor and to a dimensionless factor in Equation 9, and n is an exponent to be fit to experimental data.

2.2   Scale-Up Model.

To understand how adsorption affects both axial and radial diffusion, a model that accounts for mass transfer in the axial and radial directions, is used. Model parameters determined for laboratory-scale filters may need to be modified before they can be used to predict the performance of the full-scale filters. The second model, which will be referred to as the scale-up model, is intended to aid in determining how parameters used in the breakthrough model will change on scale-up. Neglecting fluid-phase accumulation and effects due to finite mass transfer

$$\rho_b \frac{\partial q}{\partial t} + \frac{\partial \varepsilon v c}{\partial z} - D_z \frac{\partial^2 \varepsilon c}{\partial z^2} - D_r \left[\frac{1}{r} \frac{\partial \varepsilon c}{\partial r} + \frac{\partial^2 \varepsilon c}{\partial r^2} \right] = 0 \qquad (7)$$

where D_z and D_r are effective diffusion coefficients in the axial and radial coordinate directions. These differ from D_{AB} due to packing tortuosity and eddy diffusion. The velocity, v, is dependent on the radial position. Although the velocity distribution is likely complex, use of a simplified profile may be adequate to understand scale-up effects. Fahien and Stankovic[8] derived an equation for the velocity in a packed bed based on their observation that the maximum velocity occurred one particle diameter from the wall. The velocity profile Fahien and Stankovic[8] derived is a function only of the ratio of the particle diameter and the diameter of the packed bed. The ratio is denoted by α.

Dimensional analysis allows information to be obtained from an equation without having to solve it. This is especially useful in determining scale-up effects when equations describing a process are difficult to solve. The dimensionless form of Equation 7 is

$$\frac{\partial X}{\partial \tau} + \frac{dX/dY}{\Lambda} \frac{\partial v X}{\partial \zeta} = \frac{1}{Pe_z} \frac{dX/dY}{\Lambda} \frac{\partial^2 X}{\partial \zeta^2} + \frac{1}{Pe_r} \frac{dX/dY}{\Lambda} \left[\frac{1}{\rho} \frac{\partial X}{\partial \rho} + \frac{\partial^2 X}{\partial \rho^2} \right] \qquad (8)$$

where $X = c/c_{ref}$, $Y = q/q_{ref}$, $\zeta = z/L$, and $\rho = 2r/D$. The dimensionless time is $\tau = \varepsilon v_f t/L$, where v_f is the superficial feed velocity. The axial Peclet number is defined $\varepsilon v_f L/\varepsilon D_z$, and a radial Peclet number is $Pe_r = (D/2L)(\varepsilon v_f D/2\varepsilon D_r)$ where D_z and D_r are the effective diffusion coefficients in the axial and radial directions. Dimensionless groups defined so far apply also for systems where there is no adsorption. The partition function $\Lambda = \rho_b q_{ref}/c_{ref}$ is a measure of adsorbent capacity, and dX/dY is the dimensionless derivative of the adsorption isotherm. The dimensionless velocity v is a function of radial position. The shape of the function is determined by the ratio of particle to bed diameters, α.

The dimensionless isotherm derivative is unity for a linear isotherm. This is consistent with the observation made by Mahle and Friday[5] that the Langer[3] correlation for the effective dispersion coefficient becomes more reliable when the isotherm is linear. For a linear isotherm, Equation 8 has the same form as the analogous equation describing flow through a packed-bed without adsorption (i.e., the situation the Langer[3] and Bischoff[1] correlations were formulated to

describe). For a Langmuir isotherm, the factor dX/dY evaluated at $X = Y = 1$ is equal to $1/R$, the inverse of the separation factor. This suggests a definition

$$R_1 = \frac{1}{dX/dY}\Big|_{X=1} \tag{9}$$

The effect dX/dY has on dispersion can be understood by examining the interplay between convection, axial diffusion, and radial diffusion. The dX/dY function is multiplied by each of these terms in Equation 8 but does not affect the convection term in the same way as it affects the diffusion terms. For convection, the higher the concentration, the greater the mass flux. With diffusion, the amount of material transferred is proportional to the spatial derivative of the concentration, and the derivative has a maximum at some concentration below that of the feed. When adsorption is favorable, dX/dY, evaluated at the feed concentration, is greater than dX/dY evaluated at a lower concentration. Therefore, transport through convection is not hindered as much as transport due to diffusion when the adsorption equilibrium is favorable. When axial diffusion can be neglected (and radial diffusion is limiting), dispersion will increase with increasing favorability of adsorption. If radial concentration gradients can be neglected (and axial diffusion dominates), there will be a sharpening of the breakthrough curve with increasing favorability of the isotherm.

3. ANALYSIS AND RESULTS

Experimental breakthrough data were analyzed, and the results were tabulated. Table 1 summarizes these results. To determine the capacity of the adsorbent, the stoichiometric center was estimated. The stoichiometric center, assuming a constant feed concentration, is approximated by

$$t_{1/2} \approx t_n - \frac{1}{c_f} \sum_{t_i = t_1}^{t_n} c_{t_i} \Delta t_i \tag{10}$$

where $t_1...t_n$ are times of data points, $\Delta t_i = t_i - t_{i-1}$, c_f is the feed concentration, and c_{t_i} is the concentration at t_i. The capacity of the adsorbent was calculated from the time at the stoichiometric center by

$$q = \frac{Q c_f t_{1/2}}{M_a} \tag{11}$$

where Q is the volumetric flow rate, and M_a is the mass of the adsorbent in the filter bed. A useful measure of the extent of wave spreading is the slope at the stoichiometric center

$$SCS = \left. \frac{dy}{dt} \right|_{t_{1/2}} \tag{12}$$

The slope of the natural logarithm in the low concentration limit is also of interest.

$$LCLS = \lim_{y \to 0} \frac{d\ln y}{dt} \tag{13}$$

The concentration y is in *ppmv*.

TABLE 1. Results from Analyzing Breakthrough Experimental Data

Experiment	T (C)	RH	F_d (SLPM)	$t_{1/2}$ (hr)	q (mol/kg)	q_{sat} (mol/kg)	dc/dt (mol/m^3-hr)	dlnc/dt (1/hr)	Gr.
04/04/95B	46.5	80%	12.1	42.7	1.76	2.34	2	0.41	A
04/07/95B	60.9	40%	12.1	48.4	2	3.31	1.3	0.49	B
04/10/95A	59.6	60%	18.1	30.3	1.87	2.98	2	1	C
04/12/95A	59.6	60%	33.4	14.1	1.61	2.59	2.6	0.89	A
04/13/95B	46.5	80%	12.1	40	1.65		3	0.37	C
04/14/95A	59.6	60%	12.1	54.7	2.26	3.63		0.38	D
05/26/95A	59.8	0%	12.1	47	1.94		1	0.38	C
6/27/95	51.1	90%	12.1	36.8	1.52		1.8	0.3	B
08/07/95A	58.3	0%	12.1	31.4	1.3	2.02	1.3	0.58	B

Table 1 is a partial summary of the data taken for DMMP with a 20 *ppmv* feed on a dry basis. The table lists the experiment identifier, temperature, relative humidity, and dry feed flow rate. For all experiments, the bed diameter is 3.1 *cm*, and the bed length is 3.81 *cm*. The time at the stoichiometric center was determined from Equation 10, and the loading at equilibrium with the feed, *q*, was determined from Equation 11. The slope, at the stoichiometric center defined by Equation 12, was determined by averaging values for five data points above and five data points below the stoichiometric center. The natural logarithm in the low concentration limit, defined by Equation 13, was determined by averaging over the 10 lowest concentration points with a positive slope. The general quality of the data is indicated by a letter grade. Figure 1 shows the breakthrough curves for five of the experiments.

Adsorption Equilibrium.

Adsorption isotherms were not available for DMMP on coconut shell carbon. Data for 2-hexanol on BPL activated carbon was the closest available. The Polanyi Potential theory defines a potential energy function characteristic of a given adsorbent. This provides a means of estimating an adsorption equilibrium relationship for a chemical-adsorbent pair from measured
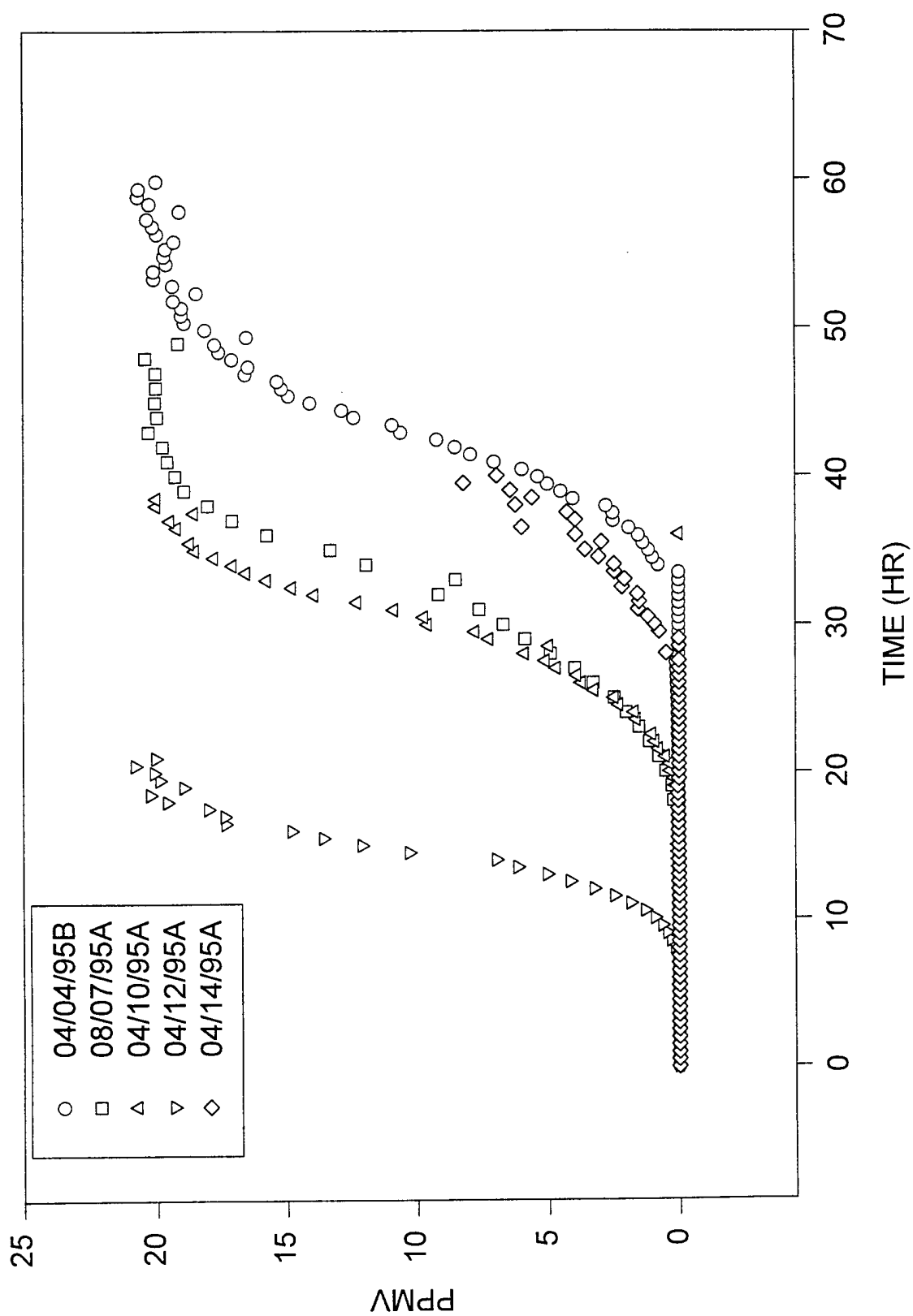
FIGURE 1: DMMP/COCONUT SHELL BREAKTHROUGH DATA

Legend:
- ○ 04/04/95B
- □ 08/07/95A
- △ 04/10/95A
- ▽ 04/12/95A
- ◇ 04/14/95A

X-axis: TIME (HR)

Y-axis: PPMV

data of another chemical on either the same or similar absorbent. The more similar the adsorption properties of the two chemical-adsorbent pairs, the more accurate the approximate adsorption equilibrium relationship can be expected to be. The Dubinin-Astakhov equation is based on the Polanyi Potential theory and may be expressed in the form

$$\ln p = \ln p_{sat} - \frac{\beta E}{RT} \left[-\ln\theta \right]^{\frac{1}{m}}$$

(14)

where the fractional loading $\theta = q/q_{sat}$. The saturation vapor pressure p_{sat} is given by the Antoine equation.   To estimate equilibrium for the DMMP/coconut shell carbon system, for which only one data point was available, the following procedure was used. Fitted values for $\beta E/R$ and m obtained for 2-hexanol on BPL carbon were reused without modification. The vapor pressure equation for 2-hexanol used to correlate BPL carbon data was changed to that for DMMP. The value of q_{sat} was fit to the DMMP/coconut shell carbon data point. Isotherm parameters fit for 2-hexanol are shown in Table 2. Except for q_{sat}, parameters estimated for the DMMP-coconut shell system are also shown in Table 2. DMMP Antoine constants were found by fitting data reported by Kosolapoff.[10]   Best fit values determined for q_{sat} were found to differ for each set of experimental conditions and are listed in Table 1.

TABLE 2. Constants used for Adsorption Equilibrium, P(Pa), T(K), q(mol/kg)

2-Hexanol/BPL Dubinin-Astakhov Constants	$q_m = 3.736$	ßE/R = 2700	$m = 2.103$
2-Hexanol Antoine Constants	A = 21.612	B = 3158.5	C = -99.98
DMMP Antoine Constants	A = 17.46	B = 1635.6	C = -184.6

The effective dispersion coefficient and the external mass transfer coefficient were fit to experimental data using the maximum likelihood approach. The simplex method was used to minimize

$$\chi^2 = \sum \frac{\left(m_i - d_i \right)^2}{\sigma_i^2}$$

(15)

where the m_i and d_i are the model predictions and the measured data at the series of times i. The variance σ^2 was assumed to be proportional to the magnitude of the breakthrough at any given time i. It was defined as

$$\sigma = \left(m_i d_i\right)^{0.5} \qquad\qquad (16)$$

The model equations were solved using an initial approximation for D_L and k_f. At every time i for which a data point was available, the model output its prediction for the breakthrough concentration at that time. When the run was complete, all information needed to evaluate Equations 15 and 16 was available.

The data first modeled was from the 04/04/95B experiment where a 20 *ppmv* DMMP feed at 80% RH was passed through a filter containing coconut shell carbon. The conditions of the experiment are listed in Table 1. For this experiment, q_{sat} was determined to be 2.34 *mol/kg*. The one dimensional breakthrough model was run with initial approximations for D_L and k_f, and breakthrough concentrations were calculated for all times for which data points were available. Equation 15 was minimized using the simplex method presented by Press and co-workers.[9] The results for selected iterations are shown in Figure 2. The final results significantly differ from the initial approximations and remain at the final values for many iterations. The fit value for the effective dispersion coefficient is $D_L = 61.1$ cm^2/s, and for external film mass transfer, $k_f a = 346$ *1/s*. The best fit of the data is shown in Figure 3.

The values for the external film mass transfer and effective dispersion coefficients were also calculated from Equations 4 and 5, assuming the values for the physical properties listed in Tables 1 and 3. The binary gas diffusion coefficient was calculated using the method of Wilke and Lee (Reference 11). The viscosity was assumed to be equal to that of air at the temperature of the 04/04/95B experiment and was taken from Appendix 9 of McCabe and co-workers.[12] The coconut shell particles range from 0.1 to 0.4 *cm* and are irregularly shaped. The shape factor used was that for anthracite coal given by Geankolis,[13] and the diameter used was the average. The resulting external film coefficient was 214 *1/s*. The calculated value for the effective dispersion coefficient was 1.8 cm^2/s. The prediction for the external film resistance was within about 40%, close to the fit value. The value predicted for D_L was 97% less than that of the fit value. The fit value for D_L was used with Equation 6 to determine the exponent $n = 1.7$.

TABLE 3: Properties used in Correlations for k_f and D_L

D_{AB}	0.085 $cm^2/$	μ	0.018 *cP*
d_p	0.2 *cm*	ϕ_s	0.63

The values of D_L and k_f fitted to experiment 04/04/95B were used with the value for q_{sat} fitted to the dry experimental data (experiment 08/07/95A) to model results for DMMP breakthrough in dry air. The result is shown in Figure 4. Early breakthrough appears to be modeled well by coefficients fitted to the previous experiment; but, in the higher concentration region, model prediction begin to deviate from the data.
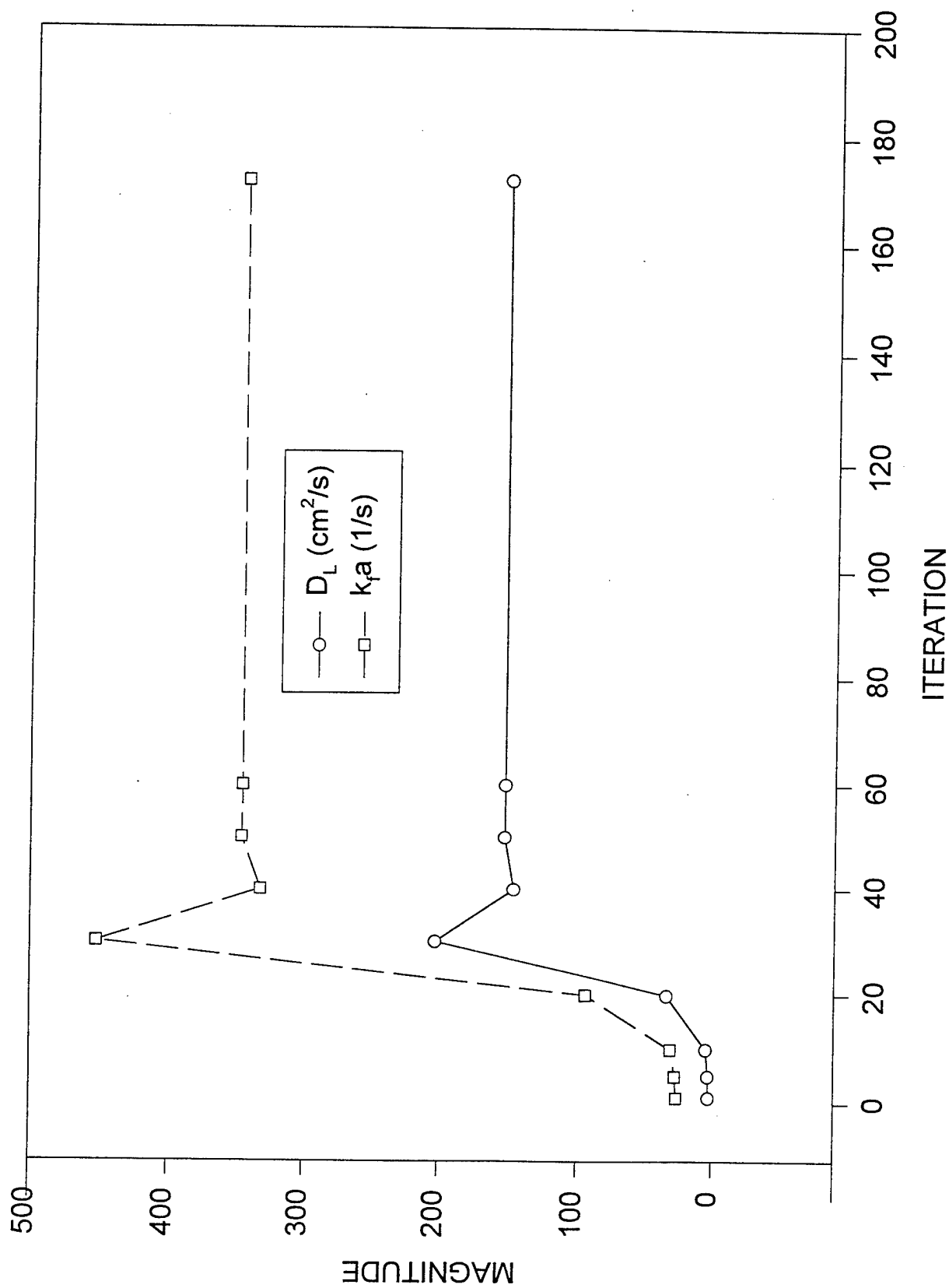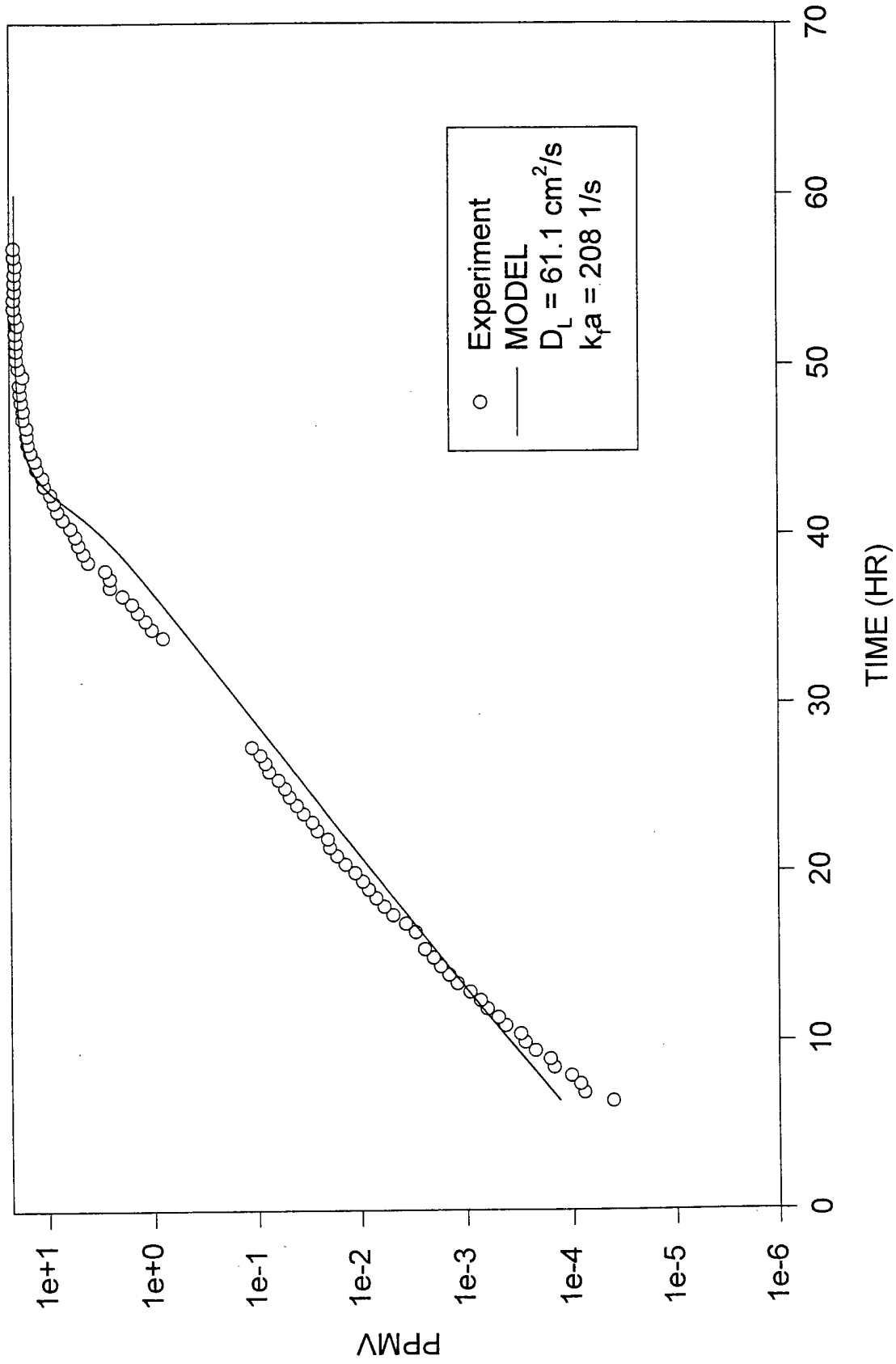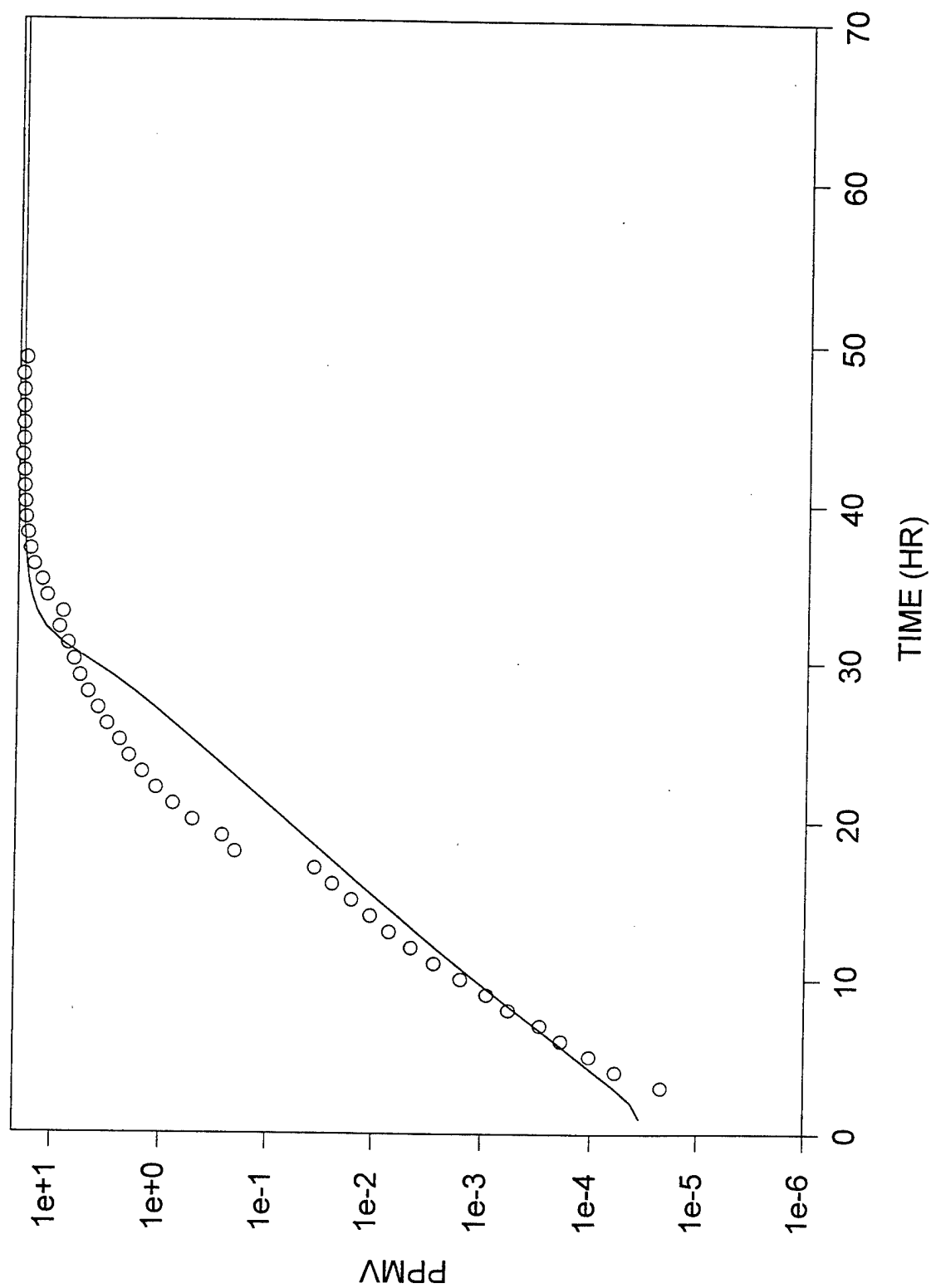
FIGURE 2: SIMPLEX FIT OF FICKIAN DISPERSION
AND EXTERNAL MASS TRANSFER COEFICIENTS

FIGURE 3: BREAKTHROUGH RUN 04/04/95B
EXPERIMENT AND LEAST SQUARES FIT MODEL

17

FIGURE 4: PARAMETERS FIT TO RUN 04/04/95B 80% RH
USED TO FIT RUN 08/07/95A 0% RH

18

Model predictions using values from Equations 4 and 6 and q_{sat} values in the isotherm equation fit to the experimentally determined stoichiometric centers are shown in Figure 5. The flow rates increase from experiments 04/14/95A, 04/10/95A, and 04/12/95A. Constants from correlations are listed in Table 4. Figure 5 shows that the slope of the logarithm of the concentration increases with increasing flow rate.

TABLE 4: Constants from Equations 4 and 6 with n = 1.7 used for Model Results for Figure 5

Experiment	Re	$k_f a$ (1/s)	D_L (cm^2/s)
04/14/95A	24.1	200	48
04/10/95A	34.7	260	73
04/12/95A	64.4	360	140

4. DISCUSSION

4.1 Breakthrough.

Figure 3 shows that the model fits the wet (80% RH) data fairly well, especially in the low concentration region. This is expected because Equation 15 is defined in such a way to emphasize the errors at low concentrations. If the earliest breakthrough that *bypasses* the adsorbent completely is chemical, then finite fluid-phase mass transfer rates as well as effective dispersion are important in this region. Note the fit value for the external film coefficient (346 $1/s$) is close to the value calculated from the correlation (214 $1/s$). The later, middle- to high-concentration breakthrough more likely consists of re-mixed chemical that had been distributed along a radially dependent concentration front before leaving the filter. In this case, the effective dispersion coefficient D_L is more important. The value for D_L calculated from the published correlation Equation 5 (1.8 cm^2/s) is 97% lower than the fit value (61.1cm^2/s). As noted, Mahle and Friday[5] found that fit values for D_L were increasingly greater than Langer correlation values[3] as adsorption isotherm favorability increased. Predictions were improved when the Langer value[3] for D_L was divided by the separation factor, R. More work is required to better establish a correlation for deviations between either the Langer[3] or similar correlations and isotherm separation factors. If D_L can be predicted from the ratio of the Bischoff correlation prediction[1] (Equation 5), and the separation factor, then the separation factor can be estimated from fit values of D_L and the Bischoff correlation prediction[1] of D_L. This ratio indicates that the separation factor for DMMP on coconut shell at 20 *ppmv* in the presence of water vapor is about 0.03. Our tentative correlation, Equation 6, predicts the fit value for D_L when n is set to 1.7.

Figure 4 compares the wet data (80% RH) fit to the dry data (0% RH). The same values for k_f and D_L were used with a refit adsorption isotherm. The new isotherm equation uses a different value for q_{sat}. The low-concentration, early breakthrough is well fit. From the correlation, Equation 4, $k_f a$ = 210 1/s, differing by only about 2% from the value calculated for the wet experiment. The later, middle- to high-concentration breakthrough data are not fit as well. The fit value of D_L for the wet experiment is too small to model the dry experimental data.
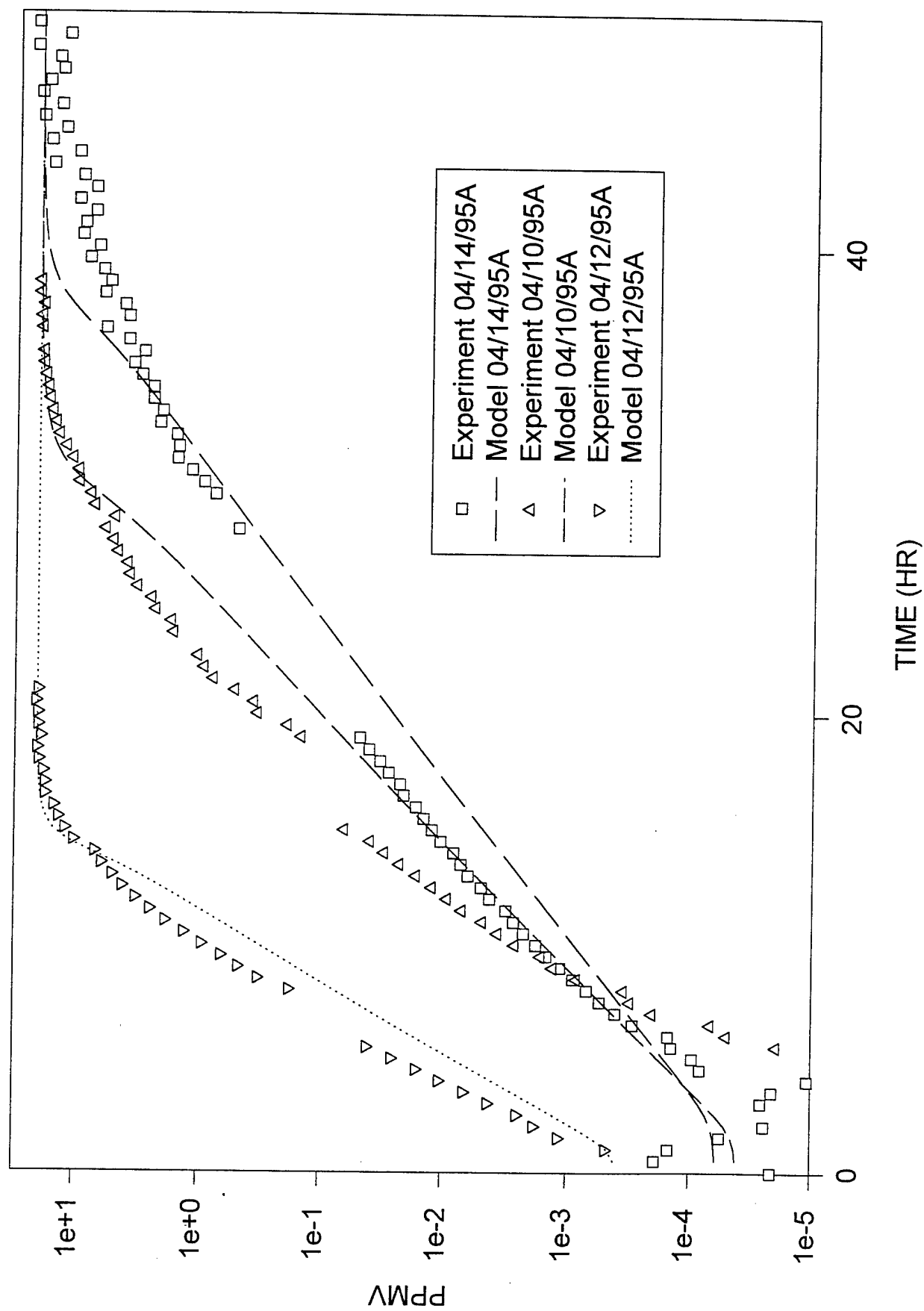
FIGURE 5: BREAKTHROUGH EXPERIMENTAL DATA AND MODEL USING EQUATIONS 4 AND 6 WITH n = 1.7

The separation factor for the dry case then appears to be smaller; therefore, the adsorption isotherm appears to be more favorable for the dry case than for the wet case. This is consistent with what one would expect.

If the early, low-concentration breakthrough is controlled by finite mass transfer rates, then reducing wall effects will not significantly affect it. The early breakthrough could be reduced by increasing the rate of mass transfer. In Figure 5, experimental and model results show that the low concentration breakthrough for the 04/14/95A case occurs before that for the 04/10/95A case even though 50% more DMMP is passed into the filter in the 04/10/95A case. This is due to the decrease in external mass transfer resistance resulting from the 50% increased feed flow rate. The middle- to high concentration breakthrough is more difficult to either predict or control. It tends to increase for a given filter with increasing flow rate. As indicated in Figure 4, middle- to high- concentration breakthrough also depends on chemical-adsorbent interactions. Equation 6 with $n = 1.7$ was used to estimate D_L. The model results fit the experimental data fairly well. However, more work is needed to develop reliable correlations for D_L as a function of the important dimensionless groups.

4.2   Scale-Up.

Dimensional analysis of the breakthrough model suggests that the Sherwood number, $Sh = \dfrac{k_f \, d_p \phi_s}{D_{AB}}$, is important in determining the shape of the breakthrough curve. The Sherwood number depends on the Reynolds number, $Re = \dfrac{\varepsilon v \rho d_p}{\mu}$, and the Schmidt number, $Sc = \dfrac{\mu}{D_{AB}\rho}$, which are independent of the filter dimensions. Therefore, the contribution made by finite mass transfer resistance to the breakthrough curve should not depend on filter size. Analysis of the scale-up model suggests that the ratio of particle and bed diameters, $\alpha = d_p / D$, the axial Peclet number, $Pe_z = \dfrac{\varepsilon v_m L}{\varepsilon D_z}$, and a radial Peclet number, $Pe_r = \dfrac{D}{4L}\dfrac{\varepsilon v_m D}{\varepsilon D_r}$, all change with changing filter dimensions. Therefore, scale-up problems may occur.

The scale-up model indicates that the shape of the adsorption isotherm will also affect the shape and propagation of the concentration wave through the filter through the $\dfrac{dX/dY}{\Lambda}$ group. The Langer[3] and Bischoff[1] correlations predict that radial diffusion reduces axial dispersion. For the breakthrough experiments, the correlations predict that the influence of axial diffusion is negligible. When adsorption is favorable, the greater the concentration at a point, the more rapidly the concentration wave moves at that point. This implies the following. If flow through a filter is uneven (if velocity depends on position on a cross section) and there is a uniform concentration front at the inlet of the filter at the initial time, then as time goes on, the velocity gradient distorts the concentration front. Some dispersion will occur and will result in there

being a radially dependent concentration gradient (where the velocity is greatest the concentration will be greatest). When adsorption is favorable, the higher concentration regions of the concentration wave move through the filter faster than the lower concentration regions. This amplifies the effect of uneven flow and therefore may increase the breadth of the breakthrough curve.

Subject to the assumptions inherent in the scale-up model, the extent of uneven flow is a function of the ratio of the particle to bed diameters. If this ratio is held constant, then increasing Pe_r will increase dispersion and result in earlier, more gradual breakthrough. However, if particle size remains the same as bed diameter is increased, the net effect on dispersion cannot be determined without solving the scale-up model equation. Later work, which will report on results found from solution of the scale-up model, will present a more detailed analysis.

5. CONCLUSIONS

The following conclusions were drawn from the study conducted:

(1)   The breakthrough model (Equation 1) can predict laboratory-scale breakthrough. This is a convection-diffusion equation for adsorption that considers external mass transfer resistance. The diffusion coefficient is replaced by an effective dispersion coefficient.

(2)   Early breakthrough cannot be predicted accurately without considering external mass transfer resistance.

(3)   When adsorption is favorable, the correlation for effective dispersion coefficient (Equation 5) becomes unreliable.

LITERATURE CITED

1. Bischoff, K.B., "A Note on Gas Dispersion in Packed Beds," *CES* Vol. 24, p 607 (1969).

2. Suzuki, M., and Smith, J.M., "Axial Dispersion in Beds of Small Particles," *Chem. Eng. J.* Vol. 3, pp 256-264 (1972).

3. Langer, G., Roethe, A., Roethe, K-P, and Gelbin, D., "Heat and Mass Transfer in Packed Beds---III. Axial Mass Dispersion," *J. Heat Mass Transfer* Vol. 21, pp 751-759 (1978).

4. Ruthven, D.M., *Principles of Adsorption and Adsorption Processes*, John Wiley and Sons, New York, NY, 1984.

5. Mahle, J.J., and Friday, D.K., "Axial Dispersion Effects on the Breakthrough Behavior of Favorably Adsorbed Vapors," F. Meunier and M. D. LeVan (Eds.), *In Adsorption Processes for Gas Separation,* Récents Progrès en Génie des Procédés Vol. 17, No. 5, (1991).

6. Wakao, N., and Funazkri, T., "Effect of Fluid Dispersion Coefficients on Particle-to-Fluid Mass Transfer Coefficients in Packed Beds," *CES*, Vol. 3, pp 1375-1384 (1978).

7. Bischoff, K.B., and Levenspiel, O., *CES* Vol. 17, p 257 (1962).

8. Fahien, R.W., Stankovic, I.M., "An Equation for the Velocity Profile in Packed Columns," *CES* Vol. 34, pp 1350-1354 (1979).

9. Press, W.H., Flannery, B.P., Teukolsky, S.A., and Vetterling, W.T., *Numerical Recipes in Fortran*, Cambridge University Press, New York, NY, 1989.

10. Kosolapoff, G.M. "Vapor Pressures and Densities of Some Lower Alkyl-phosphonates," *J. Chem. Soc.*, pp 2964-2965 (1955).

11. Reid, R.C., Prausnitz, J.M., and Poling, B.E., *The Properties of Gases and Liquids*, p 587, 4th ed., McGraw-Hill, Incorporated, New York, NY, 1987.

12. McCabe, W.L., Smith, J.C., and Harriott, P., *Unit Operations of Chemical Engineering*, 4th ed., McGraw-Hill, Incorporated, New York, NY, 1985.

13. Geankoplis, C.J., *Transport Processes and Unit Operations*, p 134, Allyn and Bacon, Incorporated, Boston, MA, 1978.

Blank

APPENDIX

PARAMETER CALCULATIONS

For the external film calculation for experiment 04/04/95B, the interstitial fluid was assumed to consist of 8% water vapor. The volumetric flow rate used was 13.1 SLPM. Intermediate quantities used in the calculation include $\varepsilon = 0.4$; $a = 6(1-\varepsilon)/\phi_s d_p = 28.6$ *1/cm*; $Re = 23.2$; $Sc = 1.98$; $Sh = 11.1$; $k_f = 7.48$ *cm/s*; $k_f a = 214$; $Pe_p = 2.47$; and $D_L = 1.8$ (Equation 5).

For experiment 04/07/95B, fluid was assumed to contain 9% water vapor, and the volumetric flow rate was 13.2 SLPM; $D_{AB} = 0.085 \, [334.1/319.7]^{1.8} = 0.092$ *cm²/s*; $\mu = 0.018$ $[334.1/319.7]^{2/3} = 0.019$ cP; $Re = 24.1$; $Sc = 1.96$; $Sh = 11.29$; $k_f a = 204$ 1/s; and $Pe_p = 2.47$ (Equation 5).

For experiment 04/10/95A, fluid was assumed to contain 8% water, and the volumetric flow rate was 19.5 SLPM; $D_{AB} = 0.085$ *cm²/s*; $\mu = 0.018$ *cP*; $Re = 34.7$; $Sc = 1.98$; $Sh = 13.6$; $k_f a = 264$ *1/s*; and $Pe_p = 2.40$ (Equation 5).

For experiment 04/14/95A, the same numbers as those used for experiment 04/07/95B were used.

For experiment 04/12/95A, fluid contained 8% water vapor, and the volumetric flow rate was 36.2 SLPM; $D_{AB} = 0.085$ *cm²/s*; $\mu = 0.018$ *cP*; $Re = 64.4$; $Sc = 1.98$; $Sh = 18.8$; $k_f a = 360$ *1/s*; and $Pe_p = 2.32$ (Equation 5).

For the Dubinin-Astakhov equation, the dimensionless isotherm derivative is

$$\frac{dY}{dX} = \frac{m\,R\,T}{\beta\,E}\left[-\frac{R\,T}{\beta\,E}\ln\frac{p}{p^{sat}}\right]^{m-1}$$

This equation gives the value of 0.13 for the correction factor R^1 of Equation 6 to describe the 04/04/95B experiment.